

ENC-2020-0355
PERFORMANCE PREDICTION SOFTWARE FOR HYBRID ROCKET MOTORS

Renato de Brito do Nascimento Filho

Maurício Sá Gontijo

Department of Aerospace Engineering, University of Brasília, St. Leste Projeção A - Gama Leste Brasília - DF 72444-240, Brazil

renatobnf@gmail.com

mauricio.sa.gontijo@gmail.com

Abstract. Hybrid rocket motors (HRMs) have great potential on becoming a widely used propulsion system. The nitrous oxide is one of the most used oxidizers in this technology, because it enables the use of a simple feeding system, due to the self-pressurizing properties of N_2O . Due to its two-phase characteristics, a correct and accurate modelling of its physics is necessary to the correct design of the motor. In addition, the grain regression, or burnback, may get time to model and, in general, it is applicable only to the target geometry. With this in consideration, a methodology for performance calculation of hybrid rocket motors is described in this work, providing a computational tool to make it accessible for propulsion engineers. In addition, it is also possible to consider a pressurized system. The software developed, Hybrid Propulsion Modeling and Design (HPMD), couples some models that describes the behavior of two key hybrid propulsion characteristics: i) the self-pressurizing feed system, and ii) the regression of the fuel grain, with a blowdown and a burnback model, respectively. In order to predict the overall performance of the motor the software is also coupled with the Chemical Equilibrium with Applications (CEA) program, to make precise internal ballistics calculation. Also, tools are provided to aid the user to design the motor, such as a propellant analysis, an injector head design and a nozzle design tool. The results from the HPMD, the trend over time of performance parameters, were compared with experimental curves from a hybrid tested motor. It has been proved to be a powerful, complete, and reliable tool for the design of hybrid rocket motors.

Keywords: Hybrid Rocket Motor, Performance Software, Blowdown, Burnback, Regression

1. INTRODUCTION

Hybrid propulsion is a type of chemical rocket propulsion where the propellants are stored in different states, usually the configuration is oxidizer in liquid phase and fuel in a solid grain. A common propellant combination is nitrous oxide/paraffin wax, the advantages of this combination is the self-pressurizing characteristics of the N_2O , that simplify the oxidizer feed system by avoiding the necessity for pressurization systems, and the high regression rate of the paraffin fuel grains, in comparison with others fuels used in hybrid propulsion. Because N_2O is a two-phase fluid at room temperature, an appropriate approach must be studied to properly model the tank blowdown process and accurately predict the mass flow rate of oxidizer to the combustion chamber. Together with the model for the tank emptying, a model for the solid fuel grain regression, or burnback, is necessary in order to allow the calculation of the motor performance parameters for the whole burn time.

There are several studied models for each of these processes, the self-pressurizing feed system and the burnback of the grain, that can be found in the literature, such as the work of Whitmore and Chandler (2010), Zimmerman et al. (2013) and Sethian (1999). This work proposes the use of a software that couples these various models in order to precisely model not just one subsystem but all the propulsion systems for the prediction of critical performance parameters, such as thrust, chamber pressure and specific impulse. The coupling of these models is the key for simulating the overall motor performance.

Some rocket propulsion softwares available nowadays, like the Solid Performance Program (SPP), the Burnsim, and the Rocstar for solid rocket propulsion, in which the last one is open source, and the Rocket Propulsion Analysis (RPA), which may be applied for every type of rocket propulsion, but it is focused on liquid engines, are useful and widely used

softwares. They provide enough design capability for these technologies, but for hybrid propulsion there is a lack of a complete computational tool to aid the designer on the project.

The results of the created model were compared with the experimental results of the hybrid test motor used to improve the design of the flight motor for the project GAMA-I (Gontijo et al, 2019), a sounding hybrid rocket from University of Brasília. The thrust and pressure curves were validated with experimental data obtained from a hot fire static test of the propulsive system. The objective of the comparison is to show that the coupling of the models is able to reproduce the performance profile of a HRM, when parameters like discharge coefficient and combustion efficiency are well characterized. A propellant analysis is also performed to aim in the selection of propellants depending on parameters such as percentage of components of the propellant, the chamber pressure, expansion pressure or area ratios, and other input variables.

Obtain the engine performance curves as close as possible to the actual behavior is an important factor for accurate mission analysis. The proposed tool is capable of providing a thrust curve that makes possible a flight path analysis very close to the real one, and this way, it is possible to make more precise preliminary adjustments during the pre-design phase of the HRM.

2. METHODOLOGY

2.1 Burnback

On hybrid motors, due to the grain regression, its thermodynamic, transport and performance parameters varies. For circular ports, which is the area of passage of the propellants, it is very simple to calculate the propagation of the port area, otherwise on complex geometries this analysis may get too hard and time consuming. A common approach to solve this problem is to develop geometrical calculations, but it is required to develop a series of equations for each kind of port. To create an algorithm to burnback all kinds of geometries, the level set method (Sethian, 1999) using the Hamilton-Jacobi equation with an initial value problem, Eq. (1), was used in this work.

$$\frac{\partial \Phi}{\partial t} + F|\nabla \Phi| = 0 \quad (1)$$

where Φ is the propagating interface function, t is the time and F is the interface propagation speed in the normal direction, as shown in Eq. (2).

As shown by (Sethian, 1999) it is needed to make viscosity and entropy considerations with partial differential equations to perform the numerical calculations correctly. In order to make these considerations, hyperbolic conservation laws were used with a first order upwind scheme.

For singularities, such as when a radius tends to zero, that creates a discontinuity in the derivative, a weak solution is required. A weak solution is a solution of a differential equation that satisfies an integral formulation of the equation. With that in mind, an entropy condition is used to solve these singularities.

Coupled with the level set method, the minimum distance function (MDF) incorporated on a squared grid was used to recognize the initial port ($\Phi = 0$) and, afterwards, the higher levels in a similar way as demonstrated by (Willcox et al., 2007), but adapted in bidimensional. Figure 1 a) displays a grain burnback example for a general star port geometry.

The fuel grain inside the combustion chamber burns normally to its port geometry, as shown in Figure 2. This normal direction is calculated as:

$$\vec{n} = \frac{\nabla \Phi}{|\nabla \Phi|} \quad (2)$$

To calculate the burning area on each level, each element of the grid that is intercepted by the port interface is analyzed and, using the Matlab's function *polyarea*, the area is calculated. The external grain circle is the final interface and when the MDF on all points reaches it, the simulation finishes. This provides the right modelling of slivers and burning time.

The grid dimensions are determined by the solid fuel external diameter. To decrease computational costs, all geometries are scaled down to a unitary radius geometry and at the end of the simulation all parameters are multiplied by a scaling factor, correcting the results. With this approach independently of the grain dimensions the results are highly accurate and reach the result relatively fast. To validate the results of the level set analysis, a comparison was made with a fully analytical geometrical analysis. The analytical burnback was made using the equations developed by Hartfield et al. (2003), of a star grain with an addition of a radius on the internal points of the star. Figure 1 a) shows a comparison of the perimeter versus the web, between a fully analytical burnback and a level set burnback and Fig. 1 b) shows the graphical burnback lines, or the levels of the level set theory.

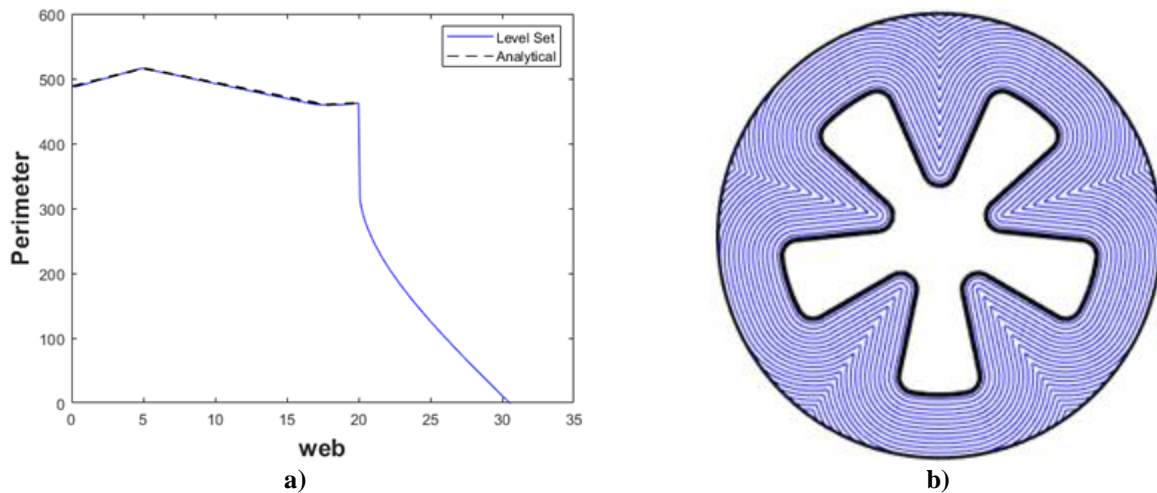


Figure 1. **a)** Grain burnback for a general star port geometry in mm. **b)** Comparison between geometrical and level set analysis

The results displayed on Fig. 1 shows that the algorithm developed predicts well the burning of the fuel grain according to previous consecrated type of analysis. It is important to mention that the analytical analysis was made excluding the sliver. Also, Fig. 1 **b)** shows that the entropy is respected and it calculates correctly the singularities, such as when the radius tends to zero. In this simulation the step was selected as a constant value of 0.1 mm. But in the full software simulation, the step is defined by the regression rate of the fuel, which varies with the burn time due to the change in the port area and the oxidizer mass flow rate, as shown in Eq, (3) and Fig. 2 displays how the regression rate acts on the regression of the grain and on the simulation.

$$\dot{r} = aG_{ox}^n x^m \quad (3)$$

where x is the distance down the port, a , n and m are regression constant and exponents obtained experimentally and function of the propellant mixture, and G_{ox} is the oxidizer mass flux, that is the oxidizer mass flow rate divided by the port area. Equation (3) is a simplified version of the Marxmans' law (Zilliac and Karabeyoglu, 2006).

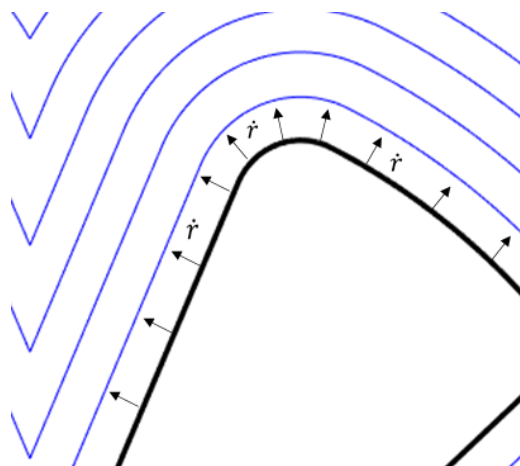


Figure 2. Level set propagation.

On Fig. 2 is possible to verify that the regression of the fuel is radially and normal to the interface, allowing to use the level set theory.

2.2 Two-phase Oxidizer Blowdown Modeling

The modeling for a two-phase blowdown process requires an engineering model for self-pressurized saturated propellant feed systems. Since N_2O is near the critical point for normal operating temperatures, N_2O cannot be assumed

to be a single-phase fluid, as a matter of fact, at room temperature it exists at both liquid and vapor phase. The assumptions of incompressible liquid and ideal gas cannot be accurately applied to model the mass-flow rate of the propellant because, as stated by (Whitmore and Chandler, 2010), the values for saturated-vapor Z factor are approximately 0.53 and for liquid compressibility Z factor are approximately 0.13. Therefore, the correct modeling of the fluid properties across the injector outlet are determinant to predict the overall performance of the propulsion system.

The models used in this work are the Nonhomogeneous Nonequilibrium (Dyer et al., 2007), Eq.(4), to predict N₂O mass flow rate and an adiabatic expansion model (Whitmore and Chandler, 2010) where the entropy of the oxidant tank at any instant during the flow, added to the entropy of the propellant portion that was discharged, equals the initial entropy in the oxidant tank. Together with this model, the properties of N₂O are calculated at each instant with the aid of thermodynamic property tables for two-phase fluids. The properties of the fluid in the tank are then calculated for every step during the blowdown by calculation of fluid quality and decrementing the tank temperature value to match the next step properties values. Equation 4 is the correction made by (Solomon, 2011).

$$\dot{m}_{out} = C_d A_{inj} \left[\left(1 - \frac{1}{1+k}\right) \sqrt{2\rho_L(P_1 - P_2)} + \left(\frac{1}{1+k}\right) \rho_2 \sqrt{2(h_1 - h_2)} \right] \quad (4)$$

where C_d is the discharge coefficient, A_{inj} is the injection area, ρ_L is the liquid density, h is the effective enthalpy of the fluid, P is the pressure and the subscripts 1 and 2 relates to the value taken upstream and downstream the injector orifice, respectively. h_i is found assuming that the fluid expands isentropically across the injector, and ρ_L is used because is assumed that the vapor pressure in the tank is sufficient to ensure that only liquid comes out of the tank and it only flashes into vapor after entering the injector orifice (Whitmore and Chandler, 2010).

The Nonhomogeneous Nonequilibrium, proposed by Dyer et al., (2007), relies on the observation that the flow regime of N₂O while crossing the injector element is somewhere between the regimes of incompressible liquid and the HEM model. Both models are incorporated in Eq. (4). The incompressible model cannot be used alone for prediction of the flow regime in this case, because of the compressible effects going on in the N₂O flow, as a result of the amount of vaporization occurring during the expansion of the fluid in the injector element. The Homogeneous Equilibrium Model (HEM) relies on the assumption of phases in equilibrium, i.e., there is no velocity difference between liquid and vapor phases (no slip between phases), but this model was evaluated and the results show it underpredicts the N₂O mass flow rate (Zimmerman et al., 2013).

Dyer model define a parameter k as a modified form of the cavitation number, which is used to build weighting factors for the mass-flow model, this number is a non-equilibrium parameter that accounts for the amount of vaporization occurring in the fluid expansion process, and depending on this value the mass-flow rate model will be better predicted using a single-phase model (the first term with the root of the Eq. (4) inside the brackets) or using a Homogeneous Equilibrium Model (the second term with the root of the Eq. (4) inside the brackets).

This weighting parameter is defined by Dyer et al., (2007) as the ratio between the bubble growth time (τ_b) and the fluid residence time (τ_r) within the injector element, as shown in Eq. (5). These two times are used to evaluate how much vaporization is occurring during the expansion of the fluid. This vaporization is a consequence of the local static pressure dropping below the vapor pressure of the fluid, causing vaporization and cavitation while the propellant is expanding in the injector orifice. The finite bubble growth rate is one of the phenomena that results in non-equilibrium effects in the N₂O injection and the two-phase injection model is built upon the measure of this rate. The parameter k is calculated as:

$$k = \frac{\tau_b}{\tau_r} = \frac{\sqrt{P_1 - P_2}}{\sqrt{P_v - P_2}} \quad (5)$$

$$\tau_b = \frac{\sqrt{1.5\rho_L}}{\sqrt{P_v - P_2}} \quad (6)$$

$$\tau_r = L \frac{\sqrt{0.5\rho_L}}{\sqrt{P_1 - P_2}} \quad (7)$$

where P_v is the vapor pressure, L is the injection port length and the constants are neglected (Dyer et al., 2007). As a saturated fluid, the properties of the propellant can be determined in function of only one thermodynamic property, in this case both temperature in the oxidizer tank and combustion chamber pressure are used, with these two values defined it is possible to obtain the values of all other thermodynamic property of the propellant, for both liquid and vapor phase, by interpolating a data sheet of properties available in the National Institute of Standards and Technology (NIST). With this data available and the calculation of the vapor mass fraction (χ) in the oxidizer tank, every property α can be calculated

with Eq. (8), where the subscripts V and L denote that the properties were evaluated for vapor and liquid phase, respectively.

$$\alpha = \alpha_V \chi + \alpha_L (1 - \chi) \quad (8)$$

Calculation of thermodynamic properties are essential in order to calculate the oxidizer mass flow rate with Eq. (4). After defining a way to calculate these properties, it is now necessary to define a model that can predict the changes in the states of the propellant in the tank while the evacuation of the oxidizer takes place. For tracking of those changes in the states of the oxidizer an engineering model is proposed by Whitmore and Chandler (2010), to enable the tank blowdown analysis.

To accurately predict the oxidizer mass flow rate, it is necessary to know the injector upstream state. During the evacuation process, part of the fluid oxidizer in the tank boils into vapor, this causes a continuous change in the vapor mass fraction, pressure and effective density within the oxidizer tank (Whitmore and Chandler, 2010).

2.3 Injector head design

To provide the required oxidizer mass flow rate and guaranteeing its atomization, a tool for the injector design is provided by the software. Through Eq. (4) the injection area may be calculated in concordance with the two-phase flow theory through the injector and, to determine the orifice diameter, atomization parameters and the choking condition are taken into consideration. The primary atomization parameter is the Reynolds number (Re), which relates the inertia and the viscosity, the second parameter is the Weber number (We), that relates the inertia and the surface tension, and the third one is the Ohnesorge number (Oh), which relates the viscosity with the droplet deformation (Gamper, 2013). The following equations shows the parameters just discussed:

$$Re = \frac{\rho_L v_{inj} d}{\mu} \quad (9)$$

$$We = \frac{\rho_L v_{inj}^2 d}{\sigma} \quad (10)$$

$$Oh = \frac{\mu}{\sqrt{\rho_L \sigma d}} \quad (11)$$

where v_{inj} is the injection velocity, d is the orifice diameter, μ is the dynamic viscosity, and σ is the surface tension. These three equations are related by the Eq. (12) and the proper values for them are displayed in the diagram of Fig. 3.

$$Oh = Re^{0.5} We \quad (12)$$

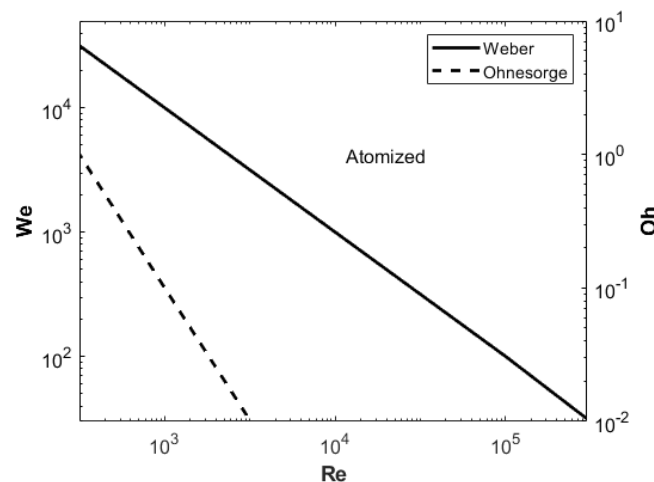


Figure 3. Weber-Reynolds-Ohnesorge diagram (Gontijo and Shynkarenko, 2020).

The choking condition assures the desired mass flow rate by forcing Mach number equal to 1 in the exit of the orifice. Reaching this condition, the oxidizer mass flow rate is dependent only by the upstream properties (Anderson, 2003). A pressure relation between the upstream and downstream is presented in Eq. (13).

$$P_1 \geq P_2 \left(\frac{2}{\gamma+1} \right)^{\gamma/(\gamma-1)} \quad (13)$$

where γ is the specific heat ratio. To characterize the flow as a choked flow, the relation shown on Eq. (13) must be followed, impacting directly on the injector design.

2.4 Internal ballistics

To perform internal ballistics calculations and predict the motor performance the software CEA (Chemical Equilibrium with Applications) (McBride and Gordon, 1994) and (McBride and Gordon, 1996) was used. The inputs for the calculations are obtained from the previous two models, burnback and blowdown. The CEA allows to make frozen or equilibrium analysis, if infinite area method is selected, or using the contraction ratio or the propellant mass flux, which are the ratio of the chamber area to the throat area and the ratio of the propellant mass flow rate and the chamber area, respectively, if the finite area method is selected. The final performance results are then calculated making some additions to CEA's results. The first addition is for the thrust coefficient, which is the pressure component in order to account for pressure difference on the nozzle exit. The second addition is the nozzle efficiency accounting for losses like drag, slip and others, also on the thrust coefficient. The last addition is for the characteristic velocity efficiency to account for the whole combustion efficiency from the injector to the nozzle throat (Gontijo and Shynkarenko, 2020).

It is also possible to make an erosion analysis providing the erosion rate. Another possibility is to provide the erosion per time curve. Erosion rate models are to be implemented in future releases. Another loss prediction possible to be used related to the nozzle throat is the discharge coefficient which represents the boundary layer displacement thickness related to the free-stream flow. This displacement reduces the effective throat area, affecting the performance of the engine. The nozzle discharge coefficient is an empirical equation and it may be calculated as:

$$C_{dN} = 1 - \left(\frac{\gamma+1}{2} \right)^{3/4} \left(\frac{-2.128}{\gamma+1} + 3.266 \right) Re_t^{-1/2} + 0.9428 \left(\frac{(\gamma-1)(\gamma+2)}{(\gamma+1)^{1/2}} \right) Re_t^{-1} \quad (14)$$

where Re_t is the Reynolds number on the throat, both properties are calculated by the algorithm automatically. The values of C_{dN} are, in general, between 0.92 and 0.99 (Hill and Peterson, 1992).

The main parameter to couple the three algorithms is the calculation of the oxidizer mass flow rate from the blowdown modeling. With this parameter calculated it is possible to calculate the fuel grain regression rate, that depends mostly on the oxidizer mass flux, and the regression rate determines the step on every Φ level so the burnback is made and all internal ballistics analysis is made for that level.

2.5 Propellant analysis

Some options for preliminary propellant analysis and selection are available. It is possible to calculate performance, thermodynamics, transport and chemical parameters for single propellant formulation, but is also possible to perform calculations varying the percentage of components of the propellant, the chamber pressure, expansion pressure or area ratios, and other input variables. Figure 4 shows one of the possible simulations available, other are ternary, contour, double Y axis, and single Y axis, providing many tools to analyze and select the propellant and engine parameters.

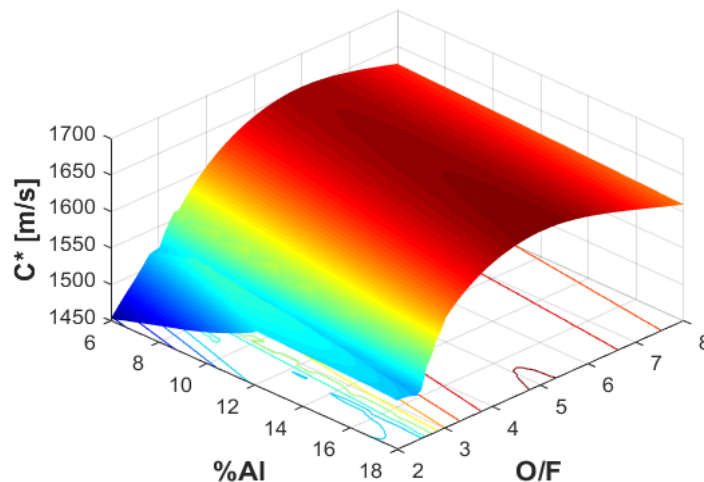


Figure 4. Surface plot for propellant analysis

On Fig. 4 it is shown a generic simulation of a N₂O/paraffin+Al propellant mixture under 40 bar of chamber pressure and it displays the influence of the percentage of content of the aluminum on the fuel grain and the mixture ratio on the characteristic velocity, enabling the user to analyze and choose a preliminary propellant formulation for the motor design.

2.6 Combustion chamber and nozzle design

The combustion chamber dimensions are regulated mainly by the fuel grain dimensions. The combustion chamber inner diameter is calculated as the grain final diameter with the addition of the liner and the thermal insulation, as shown in Eq. (15). The length is given by the grain initial length adding the pre and post combustion chambers, as shown in Eq. (16).

$$D_C = \left(\sqrt{\frac{4m_g}{\pi L_g \rho_g} + D_i^2} \right) + D_l + D_t \quad (15)$$

$$L_C = L_g + L_{pre} + L_{post} = \left[\left(\frac{\dot{m}_f n^{n-1}}{a^4 \dot{m}_p^n \rho_g} \right) D_i^{2n-1} \right]^{1/(m+1)} \quad (16)$$

where m_g is the grain mass, L_g is the grain length, ρ_g is the grain density, D_i is the initial grain diameter, D_l is the liner diameter, D_t is the thermal insulation diameter, L_{pre} is the pre chamber length, L_{post} is the post chamber length, \dot{m}_f is the initial fuel mass flow rate and \dot{m}_p is the initial propellant mass flow rate. The pre and post lengths may be given by the rule of thumb shown by Humble et al. (1995), which is given by:

$$L_{pre} \cong 0.5D_C \quad (17)$$

$$0.5D_C \leq L_{post} \leq D_C \quad (18)$$

To design the nozzle, the user may select using a conical or bell nozzle. In the case of a conical nozzle, it is required the convergent and the divergent angles, the throat and the exit dimensions are calculated by the software, and the inlet dimensions are calculated if the finite area method is selected or the user may input it. If the bell nozzle is selected, the approach available is the Rao nozzle.

The Rao nozzle is a parabolic approximation of a bell shape and was developed by Rao and discussed by (Huzel and Huang, 1992), which may be truncated in order to decrease length of the divergent part of the nozzle with the disadvantage of tabulated performance losses. The parabolic relations are also available, making it simple and fast to use.

3. HYBRID TEST MOTOR

To validate experimentally the results obtained by the software a test motor designed with the HPMD was built and tested. The motor used N₂O/Paraffin as the propellant mixture, a shower head injector, 25 bar of chamber pressure, 1.1 kN of thrust and burn time of 7.7 s. Four firing tests and cold flow tests, in which was evaluated in each one the pressure in the feed line, chamber pressure, thrust and burning time, measured by pressure transducers and load cell, respectively, were conducted. With the cold flow tests, it was also possible to evaluate the tank pressure drop during its emptying and the pressure drop in the feed line, between the tank exit and the injection manifold, it was also possible to evaluate the discharge coefficient of the injector. Figure 5 a) and b) shows the cold flow test and one of the four firing tests of the motor, respectively.

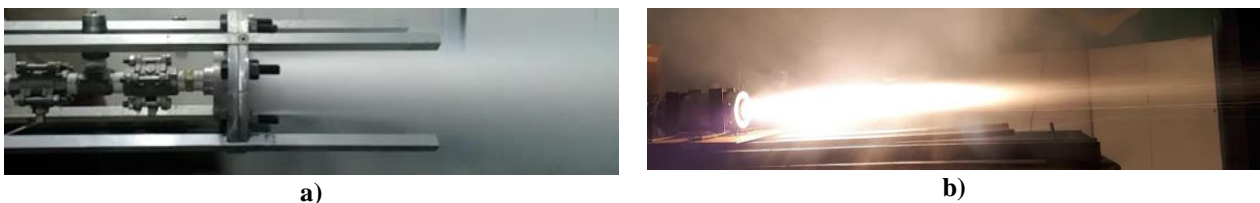


Figure 5. a) Cold flow test. b) Hot fire test

The tests were conducted on a horizontal test stand of the Chemical Propulsion Laboratory (CPL) of the University of Brasília. The performance curves obtained from this test, by the CPL's data acquisition system, was used in this work to evaluate the results obtained from the HPMD.

4. RESULTS AND DISCUSSIONS

The use of the models described can separately predict the behavior of the subsystems of the hybrid propulsion system. When put together, those models can reproduce the behavior of the overall system. Since the main parameter to integrate all the models is the calculation of the oxidizer mass flow rate (\dot{m}_{out}), the calculation of the regression rate is possible, being used in the burnback model, and the thermodynamic, transport and performance parameters are calculated. The workflow of the algorithm is illustrated below.

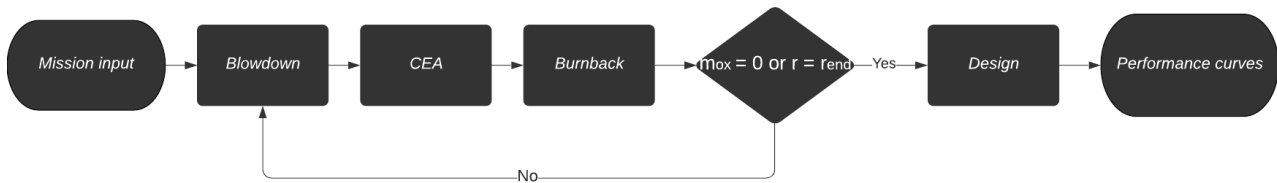


Figure 6. Algorithm workflow

On Fig. 6, it is possible to verify that the software has two stop conditions for the tank emptying loop, the end of oxidizer mass or if the port radius reaches the final radius of the grain. When any of these values are identified the loop stops and the algorithm goes to the design section, where the injector head, nozzle, and other components are designed.

After providing many analysis options for the user and all inputs are set, a plenty of plots and data are presented providing several studies and analysis possibilities. The theoretical data was also validated with experimental results. Figure 7 **a)** and **b)** shows the comparison between theoretical and experimental data of the chamber and tank pressure and the thrust, respectively. In addition, in Fig. 7 **b)** it is shown the influence of each model of the blowdown analysis.

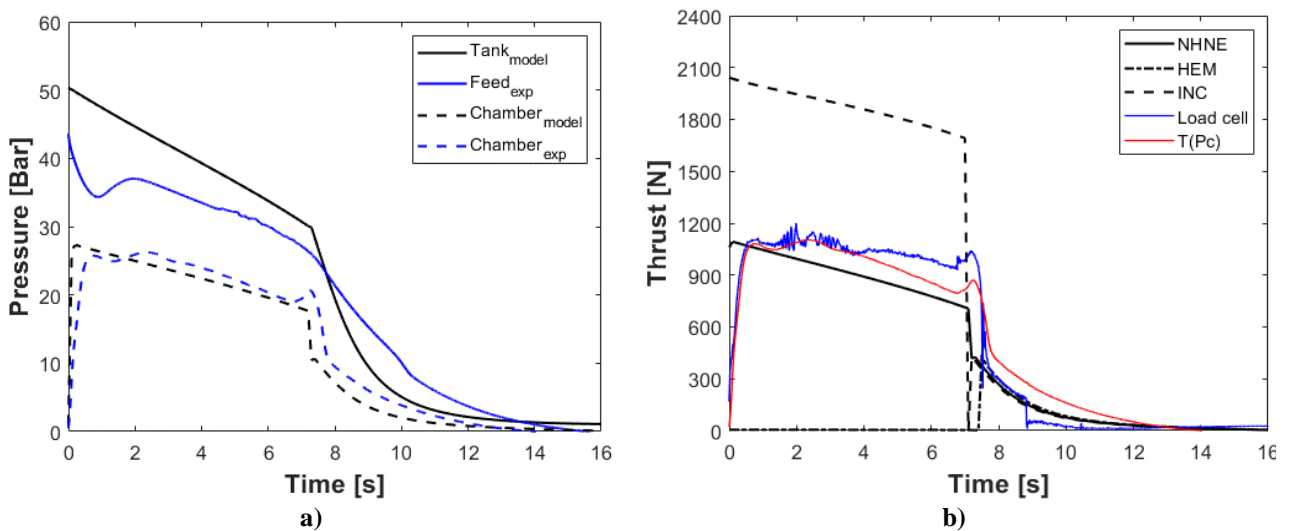


Figure 7. Results comparison **a)** Pressure curves. **b)** Thrust curves.

Analyzing the graph **a)** above, it is possible to verify a gap between experimental, measured in the feed line ($Feed_{exp}$), and theoretical tank pressure curve ($Tank_{model}$) due to the pressure drop on the feeding system between the tank and the injector. Prior tests conducted with the same motor showed a pressure drop between 2 and 10 bar on the feed line and an average discharge coefficient of 0.6 for the four firing tests. In addition, the chamber pressure ($Chamber_{exp}$) was well predicted by the HPMD ($Chamber_{model}$). Figure 7 **b)** shows how the non-homogeneous nonequilibrium model is important to model the motor performance, the incompressible model (INC) overestimate, the homogeneous equilibrium model (HEM) underestimates, and the non-homogeneous nonequilibrium model (NHNE) predicts well the results. On these curves it is also possible to verify how the weighting factor, k , works, since the HEM curve in liquid phase is close to 0 N and the INC curve close to 2000 N, and k , weights both curves to calculate correctly the oxidizer mass flow rate, and therefore the thrust.

The HPMD also predicted a bigger slope between the theoretical thrust curve (NHNE) and the experimental (Load cell) in the liquid phase, that difference between slopes can be explained by the measurements conducted during the tests, in which there were issues on fixing the load cell on the test bench. From the experimental chamber pressure curve ($Chamber_{exp}$), graph **a)**, it is possible to obtain a thrust curve ($T(Pc)$), with the relation: $T(Pc) = P_c A_i C_F$, where P_c is the

chamber pressure, A_t is the throat area, and C_F is the thrust coefficient, and it can be seen that the slopes between theoretical and experimental curves match correctly, since the thrust is dependent on the chamber pressure, it is concluded that the software showed accurate results. For this analysis the throat area was considered constant and the thrust coefficient was calculated using the CEA with the addition of the pressure difference on the exit of the nozzle term.

Both the thrust and the pressure graphs shows that the model does not calculates the chamber pressurization, that is the reason why on the beginning of the operation of the motor there is a difference between the experimental and the theoretical data.

From the thrust curve it is possible to obtain valuable information for the whole rocket project, such as total impulse, which is the integral of the thrust over time. Another important information that the blowdown analysis can give is the burn time when all the liquid N_2O is expelled from the tank and only saturated vapor remains. From the curves above, this is around 7.3 seconds, when the curve slope changes drastically, during this time the propulsion system can deliver significant thrust and, in general, the thrust generated after the liquid phase vanishes is neglected.

5. CONCLUSION

This work presented the theoretical methodology followed by the HPMD, which is a computational tool capable of design and simulate the performance of a HRM. One of the critical results obtained from the blowdown analysis is the oxidizer mass flow rate. With this key parameter is possible to calculate, for all the operation time of the motor, the performance parameters using these values for input of the burnback model, for every time step.

To prove that the software is able to make a feasible design and predict the performance of the motor in an efficient and accurate way, experimental validations with a HRM designed by the HPMD were made in a series of hot fire and cold tests. The tests data compared with the theoretical results showed that the software is reasonably precise. With this comparison, the software presented to be a powerful tool for preliminary design and performance analysis of self-pressurized or pressurized HRM, with a low computational cost. Other analyses are also available on the software, such as nozzle throat erosion, with the aim to obtain an even closer theoretical performance in relation to the real behavior of the system.

6. ACKNOWLEDGEMENTS

The authors would acknowledge the collaborators of the Chemical Propulsion Laboratory (CPL) of the University of Brasilia (UNB) for their assistance in the current research work.

7. REFERENCES

- Anderson Jr. J. D., "Modern Compressible Flow with Historical Perspective", McGraw-Hill Series in Aeronautical and Aerospace Engineering, 3rd ed., 2003.
- Dyer, J., Doran, E., Dunn, Z., and Lohner, K., "Modeling Feed System Flow Physics for Self-Pressuring Propellants," 43rd AIAA/ASME/SAE/ASEE Joint Propulsion Conference & Exhibit, AIAA Paper 2007-5702, 2007.
- Gamper E., Hink R., "Design and Test of Nitrous Oxide Injectors for a Hybrid Rocket Engine", Deutscher Luft und Raumfahrtkongress, 2013.
- Gontijo M. S., Shynkarenko O., "Investigation of a Dual-Fuel Hybrid Rocket Engine for Missile and Rocket Applications", 71st International Astronautical Congress - The CyberSpace Edition, 12-14, October, 2020.
- Gontijo M. S., Caselato A. E. L., Domingos C. H. F. L., Trindade D. B., Brandão D. A., Ribeiro G. P., Freitas L. C., Sant'ana M. S., Yamada P. Y., Silva R. F. F., Filho R. B. N., "GAMA I - Student Hybrid Rocket" 25th ABCM International Congress of Mechanical Engineering, Uberlândia, 20-25, October, 2019.
- Hartfield R., Jenkins R., Burkharter J., Foster W., "A Review of Analytical Methods for Solid Rocket Motor Grain Analysis", 39th, AIAA/ASME/SAE/ASEE Joint Propulsion Conference and Exhibit, Huntsville, Alabama, 20-23, July, 2003.
- Hill P., Peterson C., "Mechanics and Thermodynamics of Propulsion", Addison Wesley Longman, 2nd Ed. Sep 1, 1992.
- Humble R. W., Henry G. N., Larson W. J., "Space Propulsion Analysis and Design", McGraw-Hill, Sep 1, 1995.
- Huzel D. K., Huang D. H., "Modern Engineering for Design of Liquid-Propellant Rocket Engines", American Institute of Aeronautics and Astronautics, 1992.

McBride B. J., Gordon S., “Computer Program for Calculation of Complex Chemical Equilibrium Compositions and Applications”, NASA Reference Publication 1311, Part I: Analysis, 1994.

McBride B. J., Gordon S., “Computer Program for Calculation of Complex Chemical Equilibrium Compositions and Applications”, NASA Reference Publication 1311, Part II: Users Manual and Program Description, 1996.

NIST, National Institute of Standards and Technology, “Chemistry WebBook”, Jun. 2020
<<https://webbook.nist.gov/chemistry/>>.

Solomon B. J., “Engineering Model to Calculate Mass Flow Rate of a Two-Phase Saturate Fluid Through an Injector Orifice”, Master of Science, Utah State University, Utah, 2011.

Sethian J. A., “Level Set Methods and Fast Marching Methods: Evolving Interfaces in Computational Geometry, Fluid Mechanics, Computer Vision, and Materials”, Cambridge University Press; Edition: 2, 1999.

Stephen A. Whitmore and Spencer N. Chandler, “Engineering Model for Self-Pressurizing Saturated-N₂O-Propellant Feed Systems,” Journal of Propulsion and Power, Vol. 26, No. 4, 2010.

Willcox M. A., Brewster M. Q., Tang K. C., Stewart S. D., “Solid Propellant Grain Design and Burnback Simulation Using a Minimum Distance Function”, Journal of Propulsion and Power Vol. 23, No. 2, March–April 2007.

Zilliac G., Karabeyoglu M. A., “Hybrid Rocket Fuel Regression Rate Data and Modelling”, 42nd AIAA/ASME/SAE/ASEE Joint Propulsion Conference and Exhibit, Sacramento, California, 9-12, July, 2006.

Zimmerman J. E., Waxman B. S., Cantwell B. J., “Review and Evaluation of Models for Self-Pressurizing Propellant Tank Dynamics”, 49th AIAA/ASME/SAE/ASEE Joint Propulsion Conference, AIAA Paper 2013-4045, 2013.

8. RESPONSIBILITY NOTICE

The authors are the only responsible for the printed material included in this paper.